Electronic Supplementary Information

Energy Transfer and Charge Separation dynamics in Photoexcited Pyrene-Bodipy Molecular Dyads.

M. Fakis,[a,*] J. S. Beckwith,[b] K. Seintis,[a] E. Martinou,[c] C. Nançoz,[b] N. Karakostas,[c] I. Petsalakis,[d] G. Pistolis,[c,*] E. Vauthey[b,*]

[a] Department of Physics, University of Patras, 26500 Patras, Greece
[b] Department of Physical Chemistry, University of Geneva, 30 quai Ernest-Ansermet, CH-1211 Geneva, 4, Switzerland [c] NCSR "Demokritos" Institute of Nanosciences and Nanotechnology (INN) 153 10 Athens, Greece
[d] Theoretical and Physical Chemistry Institute, National Hellenic Research Foundation, Vas. Constantinou Avenue 48, 11635 Athens, Greece

Supporting Information

Table of Contents

Materials and Methods.

All chemicals purchased from commercial sources were used without further purification. $ClCH_2CH_2Cl$ and $CDCl_3$ were distilled over CaH_2, THF was distilled over Na (Ar atmosphere).

Py-Ph (1-phenylpyrene)[S1], **BD1** and **BD2** (ref. S2), **Ph-BD1** and **Ph-BD2** (ref. S3) and the parent iodophenyl-bearing Bodipy derivatives **P1** and **P2** (ref. S4) were prepared according to standard literature procedures.

All the NMR spectra were recorded on a Bruker Avance DRX 250 spectrometer. Chemical shifts are reported relative to residual solvent signals for ^{1}H (7.26 ppm) and ^{13}C (77.06 ppm) spectra.

Absorption spectra were recorded on a Perkin-Elmer Lambda-16 spectrophotometer. Steady-state fluorescence spectra were obtained by Perkin-Elmer model LS-50B and Edinburgh Instruments model FS-900 spectrophotometers.

Synthesis of 4,4,5,5-tetramethyl-2-(pyren-1-yl)-1,3,2-dioxaborolane.

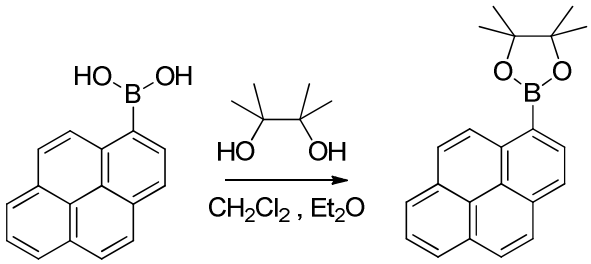

(**1**)

Pinacol (0.288 g, 2.44 mmol)) was added to a suspension of pyrene-1-boronic acid (0.5 g, 2.03 mmol) in 10 mL of anhydrous CH_2Cl_2 and 10 mL of anhydrous Et_2O. The solution was stirred for 16 h. The solvents were removed by rotary evaporation to give a light brown solid that was purified by column chromatography on silica gel (CH_2Cl_2) to 565 mg of product (1) (85% yield). ^{1}H NMR ($CDCl_3$): δ 9.07 (d, 1H), δ 8.54 (d, 1H), δ 8.23-8.00 (m, 7H), δ 1.50 (s, 12H)

Synthesis of Py-Ph-BD1.

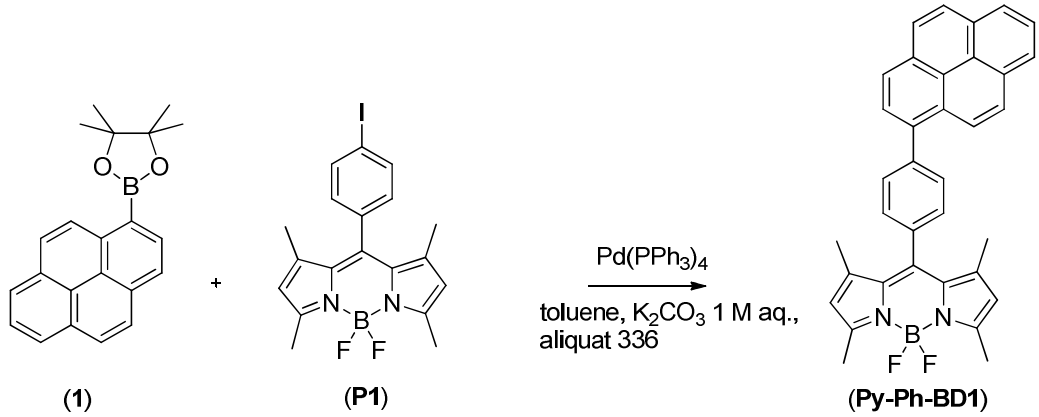

In a 50 mL flask, 4,4,5,5-tetramethyl-2-(pyren-1-yl)-1,3,2-dioxaborolane **(1)** (220 mg, 0.67 mmol) and Bodipy **(P1)** (200 mg, 0.44 mmol,) were dissolved in 15 mL toluene. Tetrakis(triphenylphosphine)palladium(0) (102.6 mg, 0.089 mmol), 1 M aqueous solution of K_2CO_3 (0.7 mL), aliquat 336 (1 drop, ca. 80 mg) were added in sequence. The reaction mixture was degassed, kept under argon, and heated to 80 °C for 24h. The solvents were removed by rotary evaporation. The product was purified by column chromatography with eluent CH_2Cl_2, hexane 1:1 to give 183 mg (yield 79%). ^{1}H NMR ($CDCl_3$): δ 8.25-8.02 (m, 9H, pyrene-H), δ 7.77 (d, 7.7 Hz, 2H, Ph-H), δ 7.50 (d, 7.7 Hz, 2H, Ph-H), δ 6.06 (s, 2H), δ 2,60 (s, 6H), δ 1,62 (s, 6H,); ^{13}C NMR ($CDCl_3$): δ 155.65, 143.16, 142.11, 136.68, 134.01, 131.52, 131.36, 130.94, 130.28, 128.14, 127.96, 12.74, 127.64, 127.46, 126.22, 125.44, 125.09, 125.04, 124.73, 124.69, 121.43, 14.68; Anal. Calcd for $C_{35}H_{27}BF_2N_2$: C, 80.16; H, 5.19; N, 5.34. Found: C, 81.45; H, 5.32; N, 5.12.

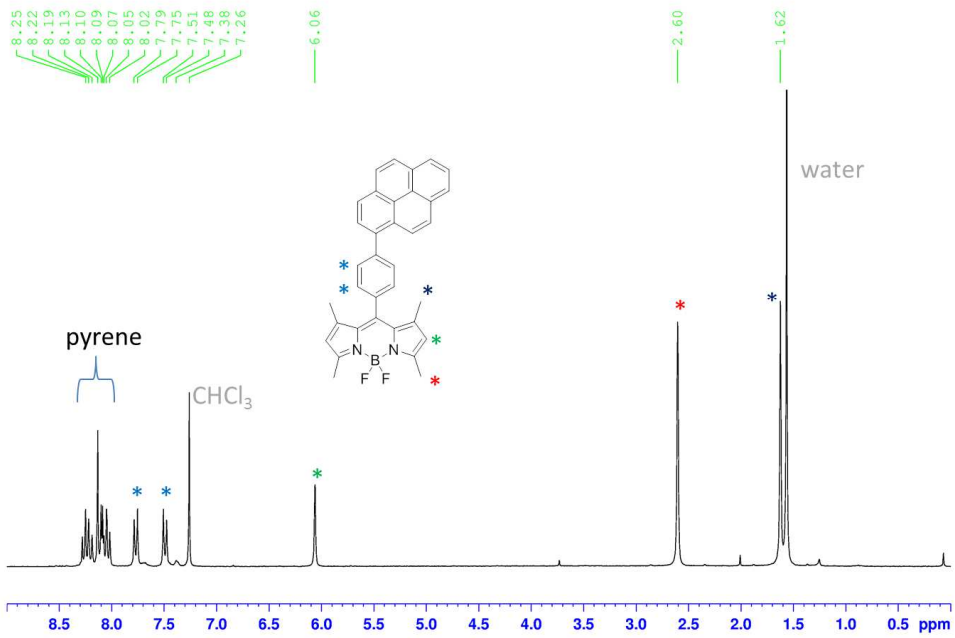

^{1}H NMR (250 MHz) spectrum of **Py-Ph-BD1** in $CDCl_3$.

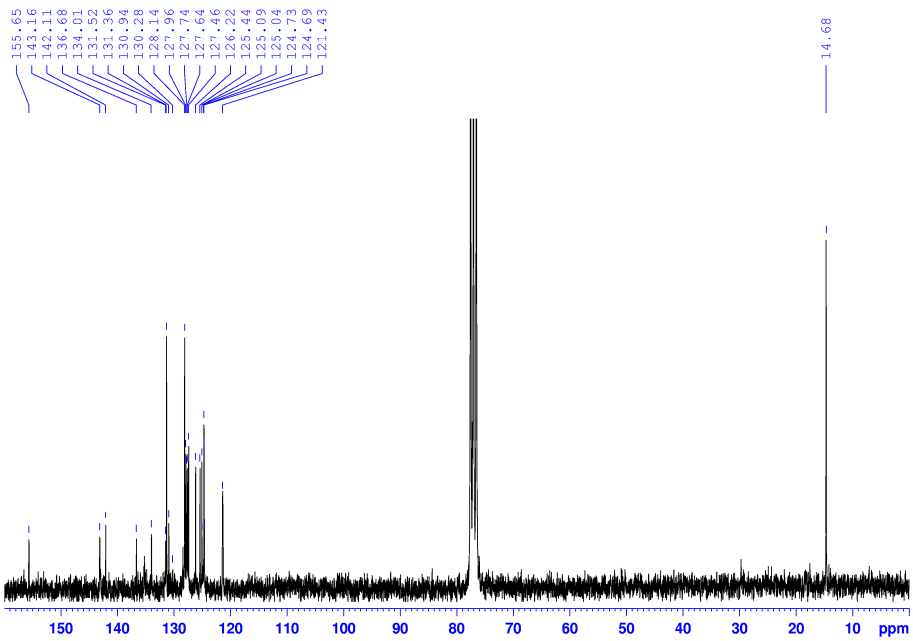

^{13}C NMR (63 MHz) spectrum of **Py-Ph-BD1** in $CDCl_3$.

Synthesis of Py-Ph-BD2.

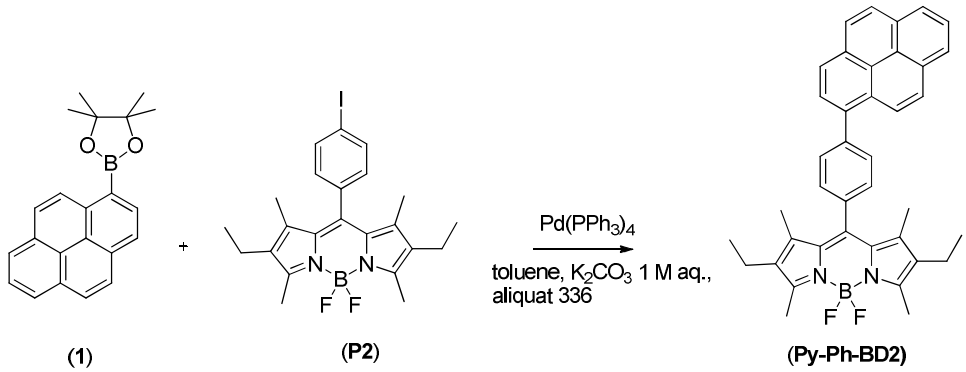

The reaction was performed in a similar way as the synthesis of Py-Ph-BD1 above: 245 mg (0.74 mmol) of 4,4,5,5-tetramethyl-2-(pyren-1-yl)-1,3,2-dioxaborolane **(1)** and 250 mg (0.49 mmol) of Bodipy **(P2)** were dissolved in 15 mL of toluene. Tetrakis(triphenylphosphine)palladium(0) (114 mg, 0.098 mmol), 1 M aqueous solution of K_2CO_3 (0.75 mL) and 1 drop aliquat 336 (ca. 80 mg) were added in sequence. The reaction mixture was degassed, kept under argon, and heated to 80 °C for 24h. The solvents were removed by rotary evaporation. The product was purified by column chromatography with eluent CH_2Cl_3, hexane 1:1 to give 242 mg (yield 84%). ^{1}H NMR ($CDCl_3$): δ 8.29-8.01 (m, 9H, pyrene-H), δ 7.76 (d, 7.3 Hz, 2H, Ph-H), δ 7.49 (d, 7.3 Hz, 2H, Ph-H), δ 2.58 (s, 6H), δ 2.37 (q, 7.2 Hz, 4H -CH2-), δ 1.53 (s, 6H,), δ 1.04 (t, 7.2 Hz, 6H, -CH3); ^{13}C NMR ($CDCl_3$): δ 153.88, 141.88, 140.02, 138.44, 136.85, 134,84, 132.97, 131.53, 131.26, 130.95, 130.92, 128.45, 127.93, 127.71, 127.66, 127.47, 126.20, 125.42, 125.07, 124.91, 124.77, 124.73, 17.20, 14.73, 12.61, 12.00; Anal. Calcd for $C_{39}H_{35}BF_2N_2$: C, 80.69; H, 6.08; N, 4.83. Found: C, 82.00; H, 6.22; N, 4.55.

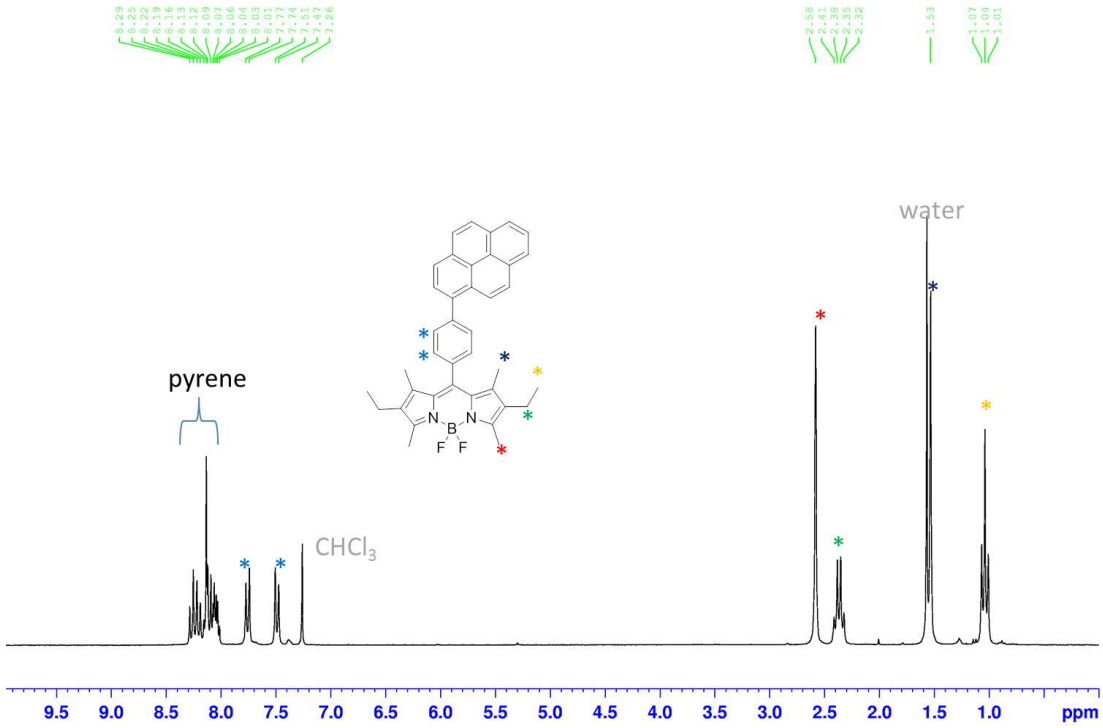

^{1}H NMR (250 MHz) spectrum of **Py-Ph-BD2** in $CDCl_3$.

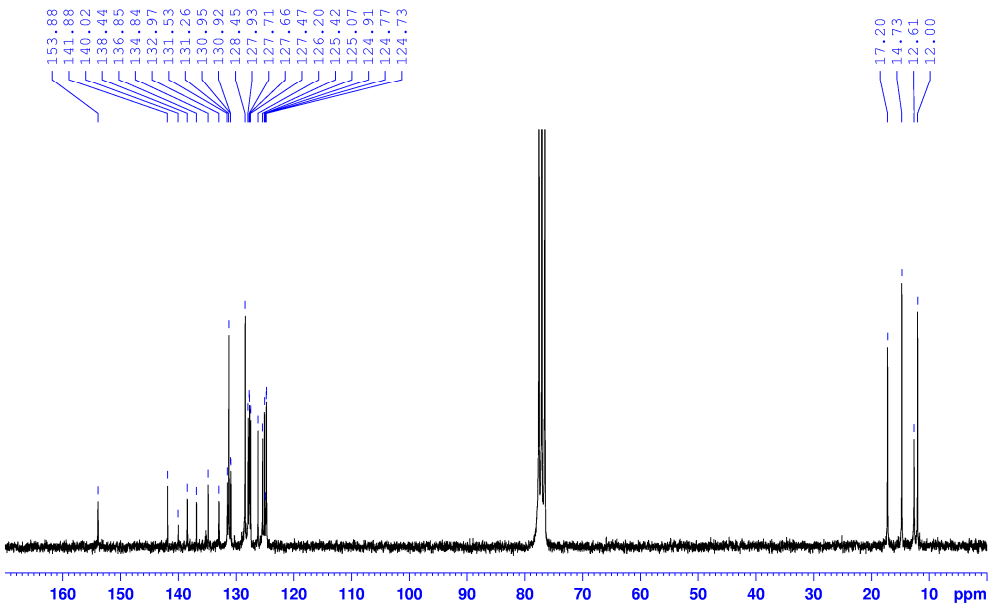

^{13}C NMR (63 MHz) spectrum of **Py-Ph-BD2** in $CDCl_3$.

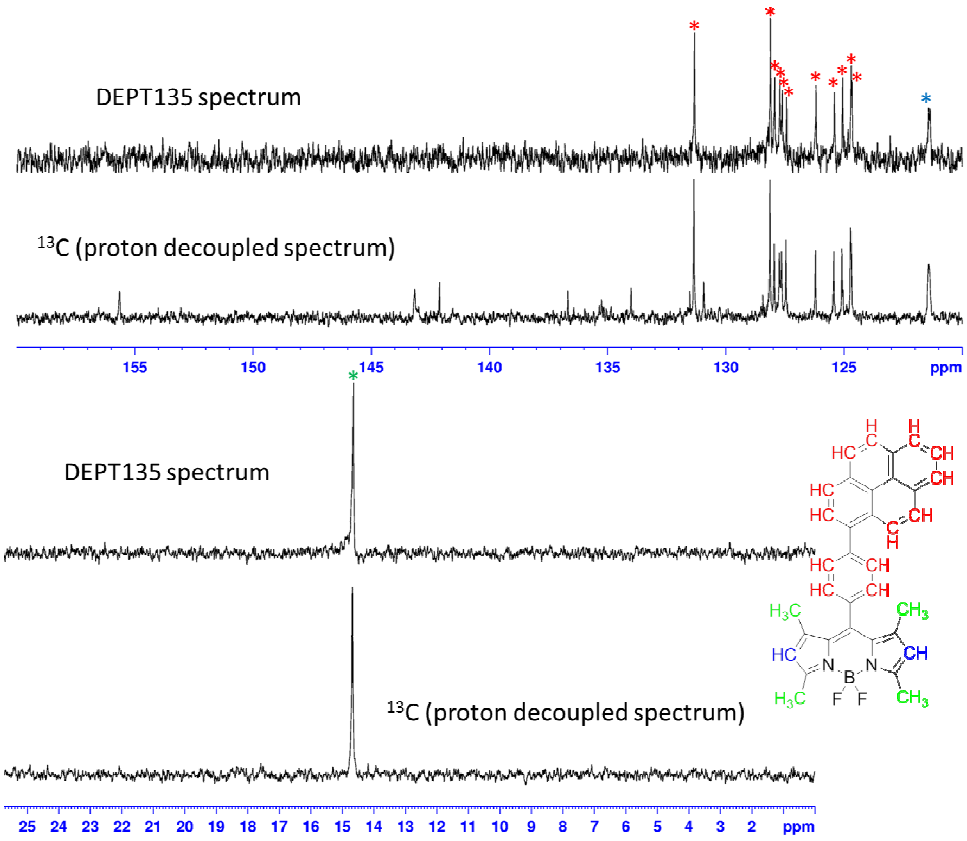

DEPT135 NMR spectrum of of **Py-Ph-BD1** in $CDCl_3$

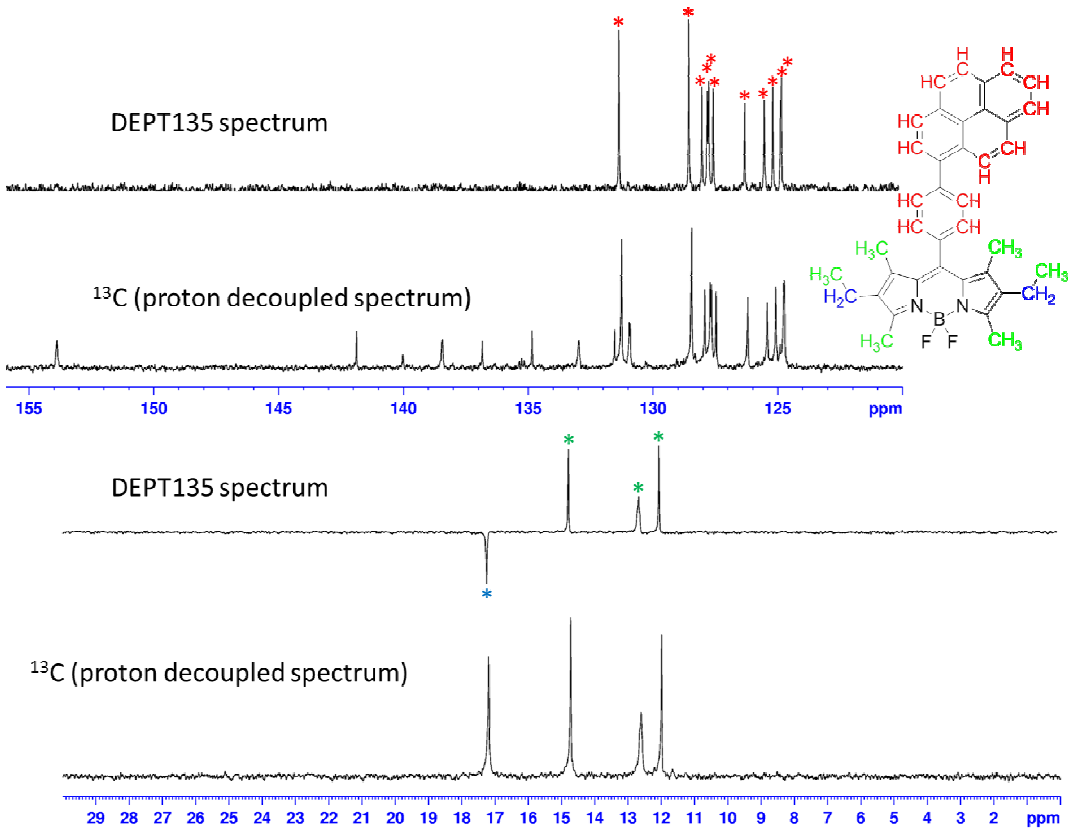

DEPT135 NMR spectrum of of **Py-Ph-BD2** in $CDCl_3$

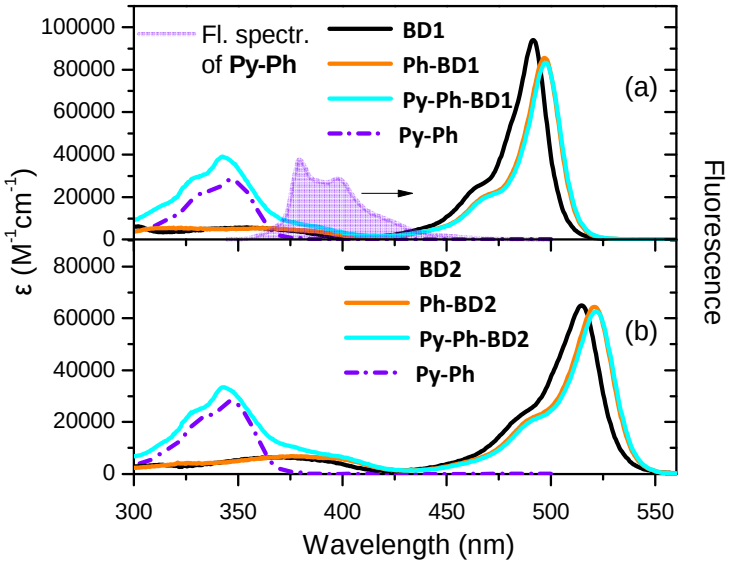

Figure S1. Electronic absorption spectra of the dyads (a) **Py-Ph-BD1** and (b) **Py-Ph-BD2** and of the individual constituents in ACN. Spectral overlap between the emission spectrum of **Py-Ph** alone (donor) and the absorption spectra of **BD1** and **BD2** (acceptors) is also shown.

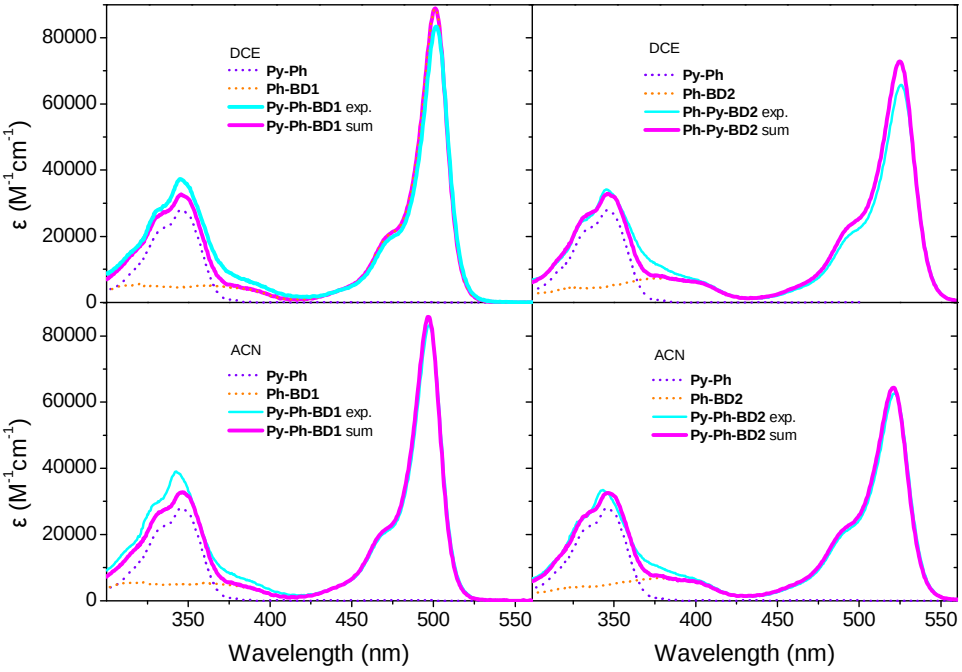

Figure S2. Comparison of the experimentally measured absorption spectra of **Py-Ph-BD1** and **Py-Ph-BD2** with those produced by the sum of the absorption of the constituent molecules.

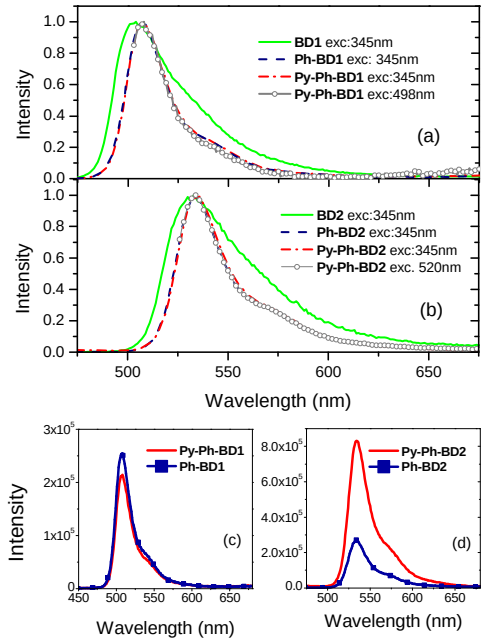

Figure S3. Normalized fluorescence spectra of (a) **Py-Ph-BD1** and (b) **Py-Ph-BD2** and reference compounds in ACN with different excitation wavelengths, (c) and (d) non-normalized fluorescence spectra of the dyads and reference compounds upon 347 nm excitation.

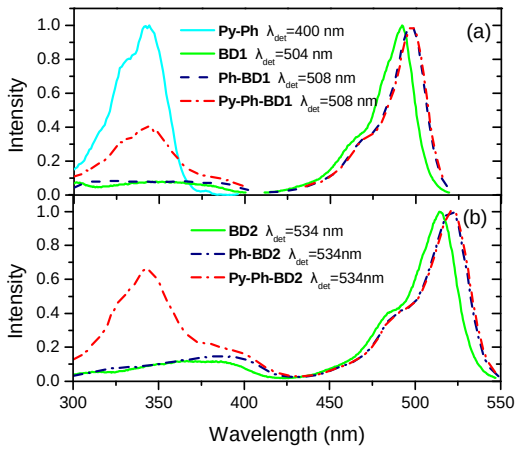

Figure S4. Excitation spectra of (a) **BD1**, **Ph-BD1** and **Py-Ph-BD1** and of (b) **BD2**, **Ph-BD2** and **Py-Ph-BD2** in ACN with detection at the **BD** emission band. Figure (a) also shows the excitation spectrum of **Py-Ph**.

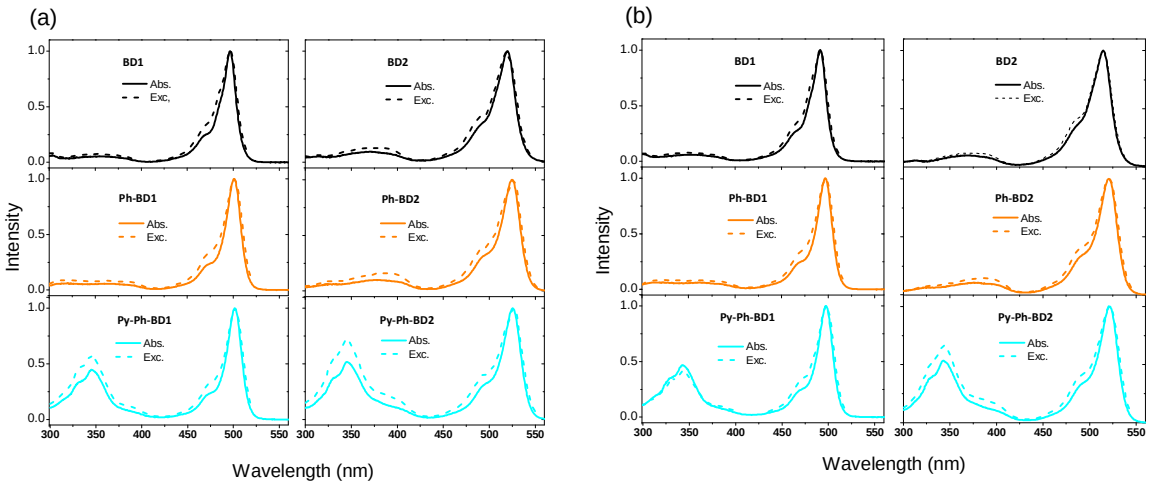

Figure S5. Comparison of the fluorescence excitation (dashed lines) and absorption (solid lines) spectra of the herein studied molecules in (a) DCE and (b) ACN.

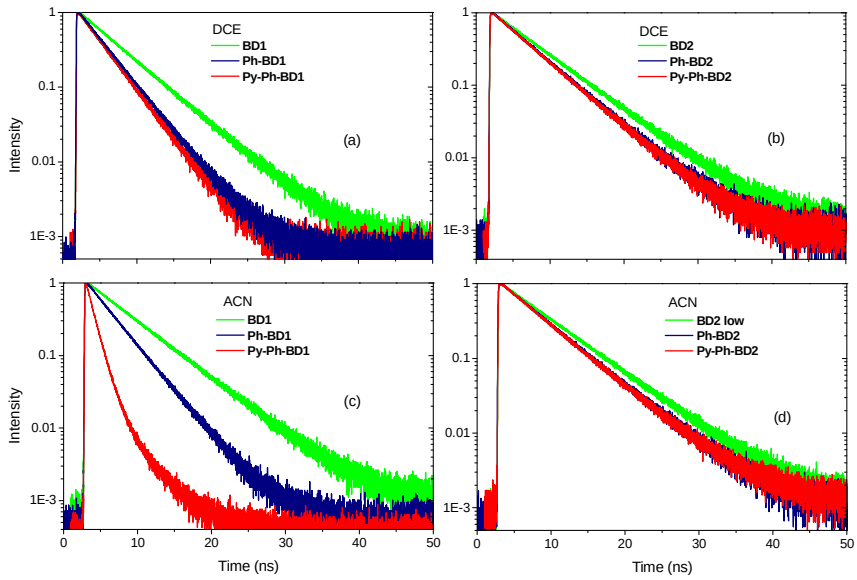

Figure S6. TCSPC dynamics for **BD1**, **Ph-BD1** and **Py-Ph-BD1** in DCE (a) and ACN (c) and for **BD2**, **Ph-BD2** and **Py-Ph-BD2** in DCE (b) and ACN (d).

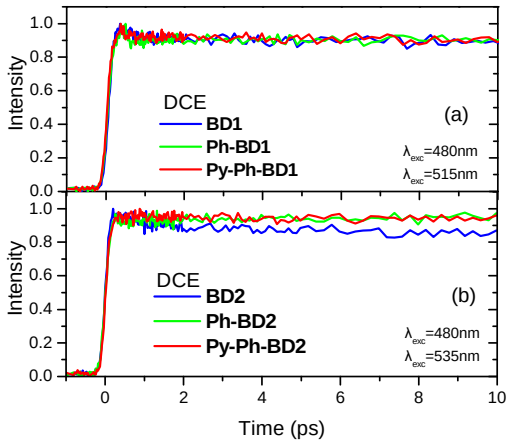

Figure S7. Fluorescence dynamics of (a) **BD1**, **Ph-BD1** and **Py-Ph-BD1** (b) **BD2**, **Ph-BD2** and **Py-Ph-BD2** in DCE upon excitation at 480 nm and detection in the Ph-BD $S_1 \rightarrow S_0$ emission band.

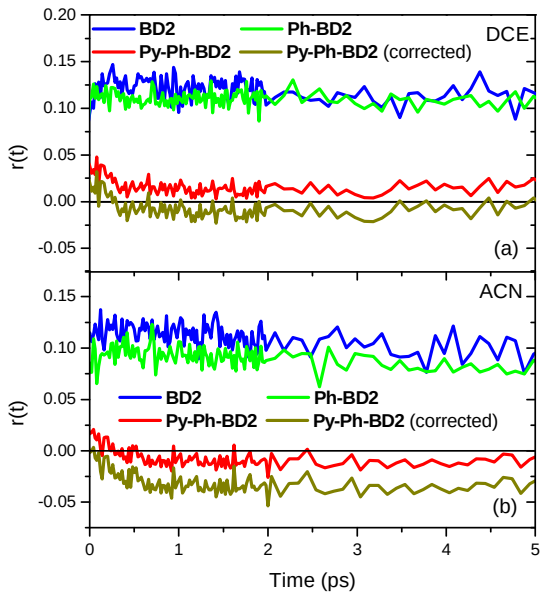

Figure S8. Anisotropy dynamics of **BD2**, **Ph-BD2** and **Py-Ph-BD2** in (a) DCE and (b) ACN upon excitation at 355nm and detection of the emission at 535 nm. The corrected anisotropy of **Py-Ph-BD1** is also shown after taking into account direct excitation of **Ph-BD1** at 355 nm.

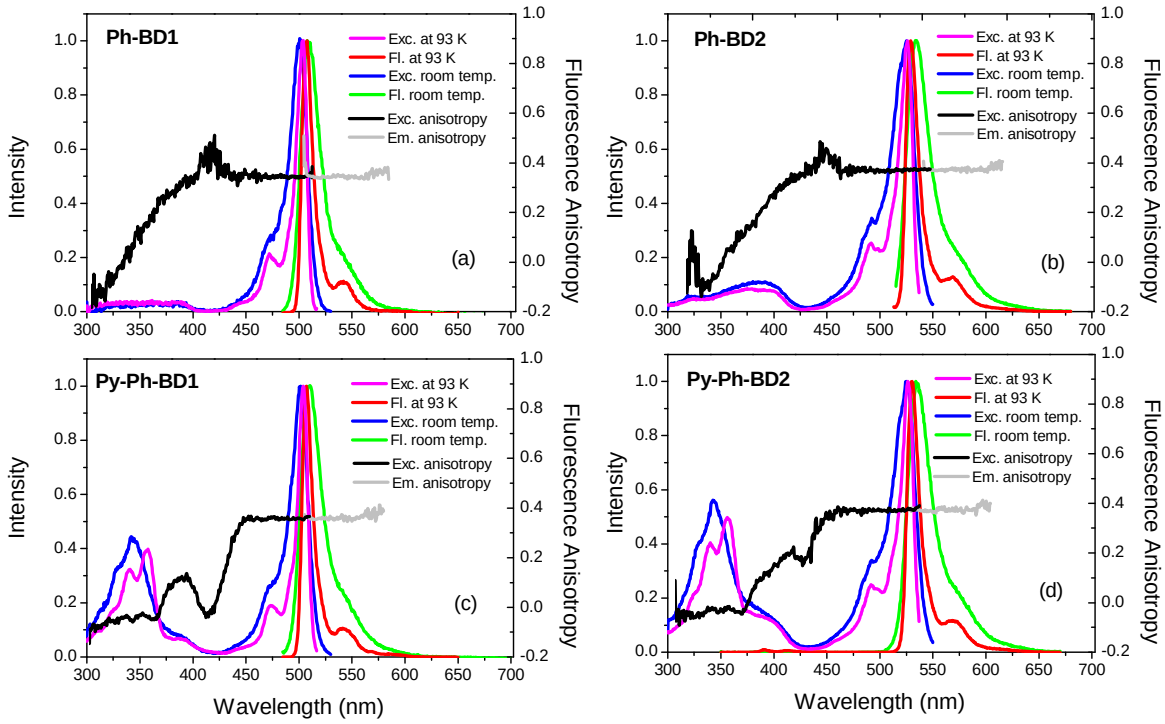

Figure S9. Low temperature (93 K) and room temperature excitation and fluorescence spectra of (a) **Ph-BD1**, (b) **Ph-BD2**, (c) **Py-Ph-BD1** and (c) **Py-Ph-BD2** in 2-MTHF. Also, plots of the fluorescence anisotropy (r) versus the excitation (black curves) and emission (grey curves) wavelength are shown.

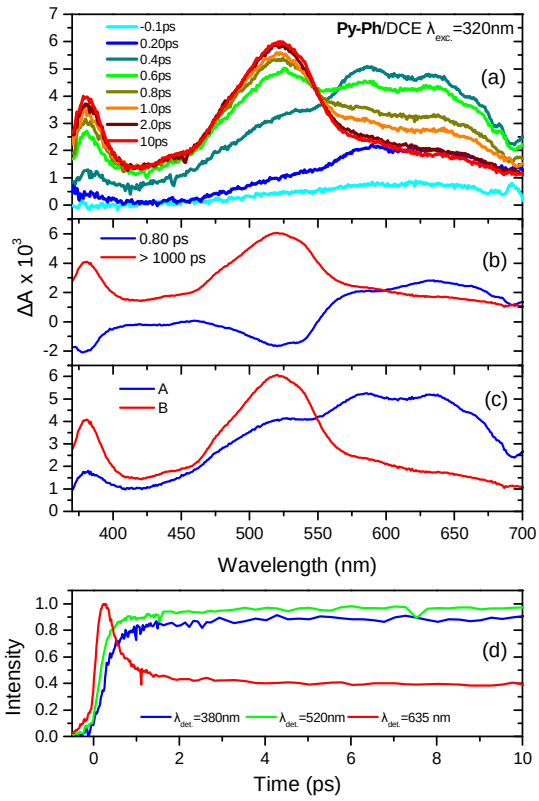

Figure S10. (a) Transient absorption spectra of **Py-Ph** in DCE upon excitation at 320 nm, (b) and (c) DADS and SADS obtained from a multiexponential analysis, (d) comparison of the intensity-normalized TA profiles at 380, 520 and 635 nm.

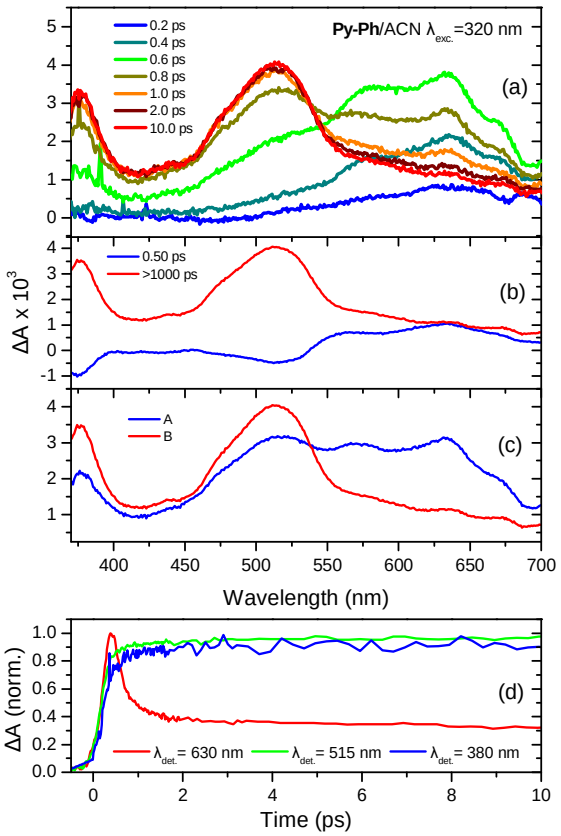

Figure S11. (a) Transient absorption spectra of **Py-Ph** in ACN upon excitation at 320 nm, (b) and (c) DADS and SADS obtained from a multiexponential analysis, (d) comparison of the intensity-normalized TA profiles at 380, 520 and 635 nm.

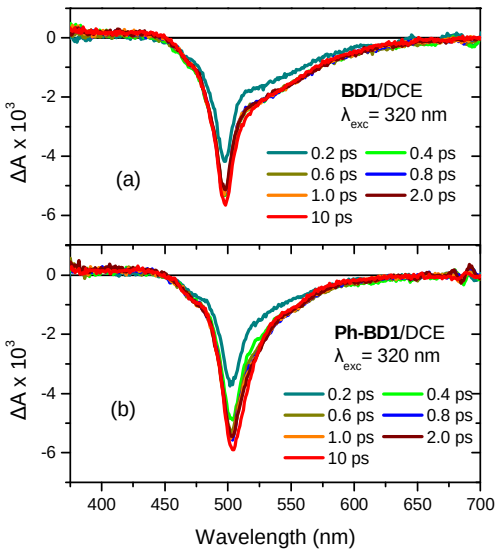

Figure S12. Transient spectra of (a) **BD1** and (b) **Ph-BD1** in DCE upon excitation at 320 nm.

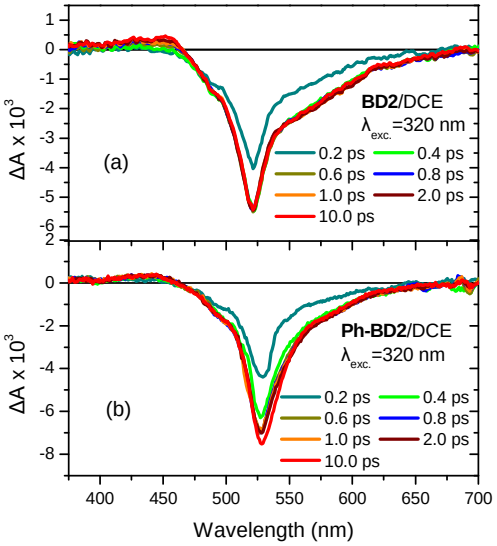

Figure S13. Transient spectra of (a) **BD2** and (b) **Ph-BD2** in DCE upon excitation at 320 nm.

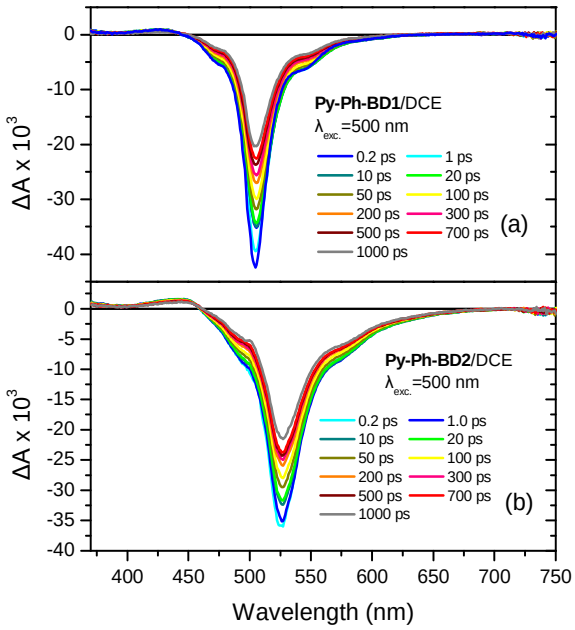

Figure S14. Transient spectra of (a) **Py-Ph-BD1** and (b) **Py-Ph-BD2** in DCE upon excitation at 500 nm.

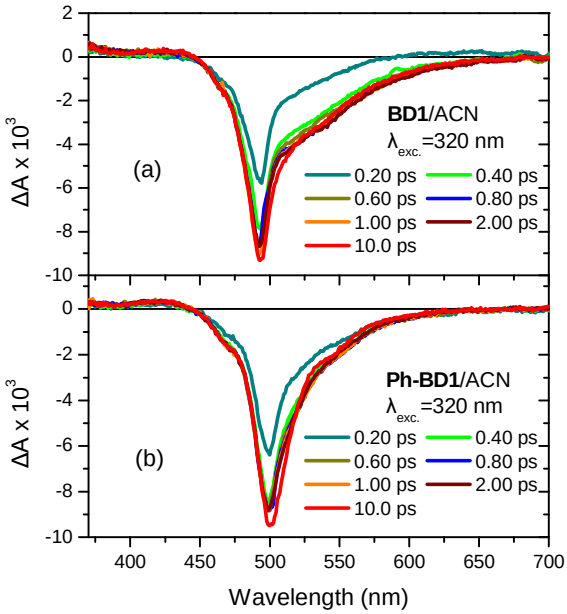

Figure S15. Transient spectra of (a) **BD1** and (b) **Ph-BD1** in ACN upon excitation at 320 nm.

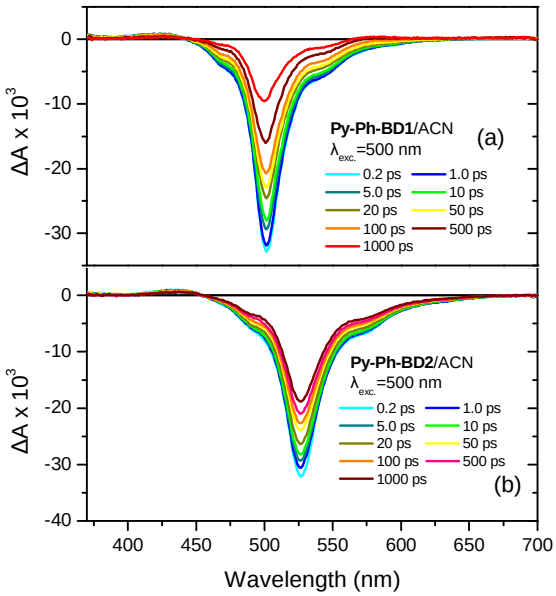

Figure S16. Transient spectra of (a) **Py-Ph-BD1** and (b) **Py-Ph-BD2** in ACN upon excitation at 500 nm.

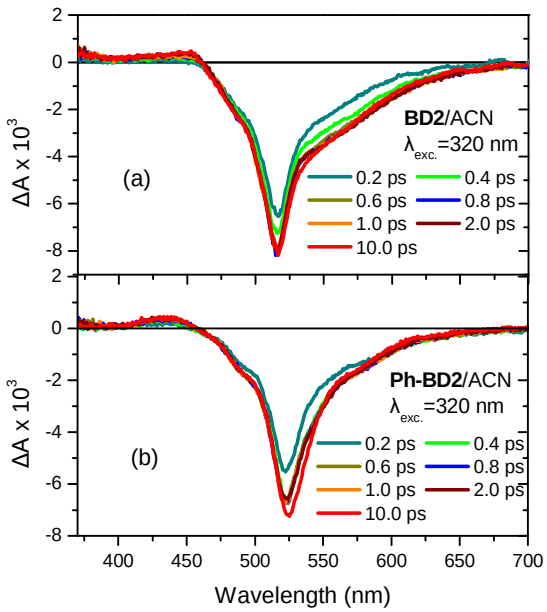

Figure S17. Transient spectra of (a) **BD2** and (b) **Ph-BD2** in ACN upon excitation at 320 nm.

Dipole – dipole Förster formulation

The overall EET rate constant between two weakly coupled chromophores can be expressed as:[S5, S6]

$$k_{EET} = k_C + k_e = \frac{2\pi}{\hbar}(V_c^2 + V_e^2)J_{DA} \quad \text{(S1)}$$

where V_C and V_e are the Coulombic and exchange interaction energies, respectively, and J_{DA} is the spectral overlap integral calculated through the area-normalized emission and absorption bands of the energy donor (D) and acceptor (A), respectively. The overlap integral J_{DA} can be expressed in terms of an overlap between donor emission, f_D, and acceptor absorption, a_A, spectra which have been each normalized to unity area on an energy scale e.g., cm^{-1}.

$$J_{DA} = f_D a_A \quad \text{(S2)}$$

The EET time constant predicted by the dipole – dipole (Förster) interactions is found through eq. S3, that relates the donor – acceptor EET rate constant k_C to the spectral overlap integral J_{DA} and the electronic coupling *Vc* for Coulombic interactions between the donor emission ($D^* \rightarrow D$) and acceptor absorption ($A \rightarrow A^*$) transition moments μ_D and μ_A at a distance R_{DA}.

$$k_C = \frac{2\pi}{\hbar}|V_C|^2 J_{DA} \quad \text{(S3)}$$

The strength of Coulombic interactions *Vc* between donor (*D*) and acceptor (*A*) transition dipoles is given by the equation:

$$V_{C(calc.)} = \frac{1}{4\pi\varepsilon_0}\kappa\frac{|\mu_D||\mu_A|}{R_{DA}^3} \quad \text{(S4)}$$

It is a function of the magnitudes of the transition dipoles μ_D, μ_A, distance R_{DA} and orientation, expressed by the κ factor given by the equation:

$$\kappa^2 = (cos\theta_{DA} - 3cos\theta_D cos\theta_A)^2 \quad \text{(S5)}$$

In the above expression, θ_{DA} is the angle between the donor's emission and acceptor's absorption transition moment while θ_D and θ_A are the angles between these dipoles and the intermolecular separation vector R_{DA} joining the centroids of the donor and the acceptor.

The transition dipole moments (μ) for the $S_0 \rightarrow S_1$ transition of **Py-Ph** (5.6 D) and of **Ph-BD1** (6.5 D) and **Ph-BD2** (6.5 D) as well as of the $S_0 \rightarrow S_2$ of **Ph-BD1** (2.6 D) and **Ph-BD2** (3.3 D) were calculated from the absorption spectra using the relation of the dipole strength:[S7]

$$D = |\mu|^2 = 9.186x10^{-3}nf^{-2}\int\frac{\varepsilon(v)}{v}dv \quad \text{(S6)}$$

where n is the refractive index and $f = 3n^2/(2n^2+1)$ is the local-field correction factor.

The center-to-center distance between the pyrene and Bodipy moiety was calculated to be about 10 Å in both dyads using the energy minimized structure. This distance is small and the point-dipole approximation can only provide us indicative results.

Calculations of the energy of the CSS, E_{CSS}, and the driving force for CS, ΔG_{CS}

Assuming charge separation from **Ph-Py** to the excited **Ph-BD** i.e. hole transfer, the energy of the CSS has been calculated using the Weller equation:[S8]

$$E_{CSS} = E_{ox}(D) - E_{red}(A) + C + S \quad \text{(S7)}$$

$$\Delta G_{CS} = E_{CSS} - E_{00} \quad \text{(S8)}$$

where $E_{ox}(D)$ and $E_{red}(A)$ are the oxidation and reduction potentials of the electron donor and acceptor groups respectively and E_{00} is the energy of the singlet excited state from which CS takes place. C is a work term taking into account the Coulombic interaction of the charges and is given by the equation:

$$C = -\frac{e^2}{4\pi\varepsilon_0\varepsilon_s d_{DA}} \quad \text{(S9)}$$

where d_{DA} is the separation distance of the charges and ε_s is the dielectric constant of the solvent used. Finally, S is a correction term accounting for the case where the E_{CSS} is calculated in a different solvent than that used for the measurements of the redox potentials:

$$S = -\frac{e^2}{8\pi\varepsilon_0}\left(\frac{1}{r_D} + \frac{1}{r_A}\right)\left(\frac{1}{\varepsilon_{s,pol}} - \frac{1}{\varepsilon_s}\right) \quad \text{(S10)}$$

where r_D and r_A are the radii of the electron donating and accepting groups, $\varepsilon_{s,pol}$ is the dielectric constants of the solvents used in the electrochemical experiments and ε_s is the dielectric constant of the solvent where the E_{CSS} is calculated.

The oxidation potential for Ph-Py was measured by cyclic voltammetry and found 1.21 V vs. SCE, while the reduction potentials of **Ph-BD1** (E_{red}=-1.19 V vs. SCE) and **Ph-BD2** (E_{red}=-1.27 V vs. SCE) were found in the literature.[S9] E_{00} was calculated by $(E_{abs(max)}+E_{em(max)})/2$ and is the energy of the S_1 state of BD subunits since CS is assumed to take place after EET. This is supported by the fact that the quenching of the S_1 state is also observed upon direct excitation of the BD unit. The radii used for the calculation of S, were found $\boldsymbol{r_{BD1}}$= 3.80 Å, $\boldsymbol{r_{BD2}}$=4.11 Å and $\boldsymbol{r_{Ph-Py}}$= 3.98

Å by using Hyperchem software. The following values have been also used: $\varepsilon_{s,pol} = \varepsilon_{ACN} = 37.5, \varepsilon_s = \varepsilon_{DCE} = 10.4$ and $d_{DA} = 10\ \mathring{A}$.

DFT and TD-DFT calculations

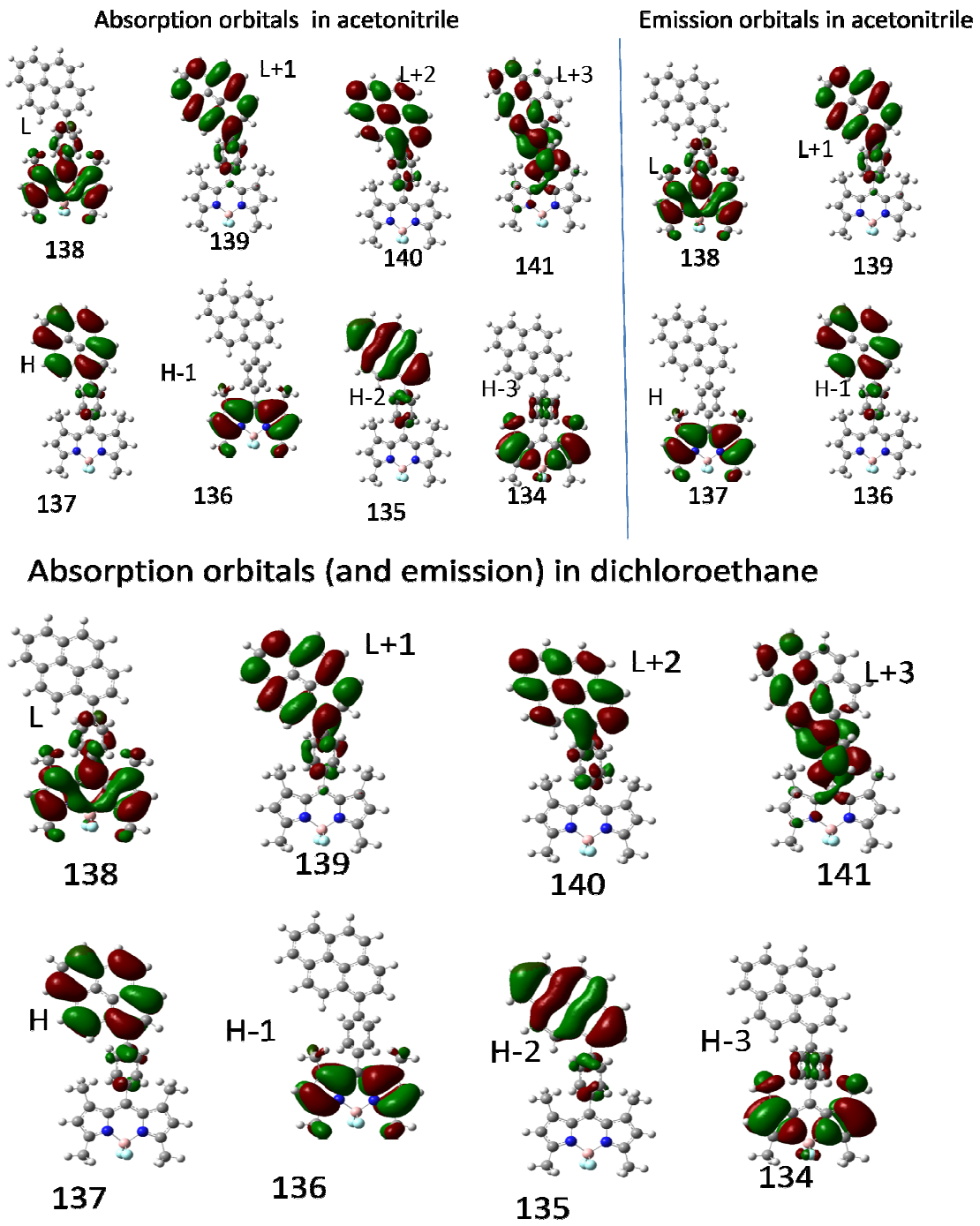

Figure S18. Molecular orbitals for the **Py-Ph-BD1** system. In DCE, MOs are the same at the absorption and emission geometry.

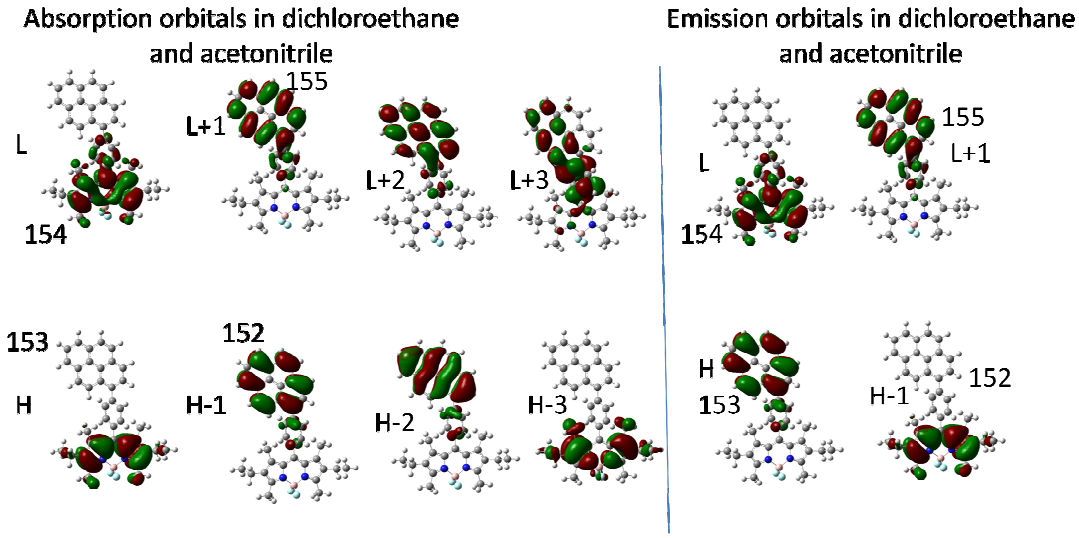

Figure S19. Molecular orbitals for the **Py-Ph-BD2** system.

The first three excited electronic states for the Py-Ph-BD1 system in DCE at the absorption geometry. (from g09 output, numbers with % gives the contribution of the actual configuration to the exited state wave function)

Excited State 1: Singlet-A 2.7217 eV 455.53 nm f=0.7625 <S**2>=0.000

136 ->138 0.70133 98%

Excited State 2: Singlet-A 3.6765 eV 337.23 nm f=0.4743 <S**2>=0.000

133 ->138 0.20020 8%

137 ->138 0.55530 61%

137 ->139 0.36317 26%

Excited State 3: Singlet-A 3.8067 eV 325.70 nm f=0.6388 <S**2>=0.000

133 ->138 -0.12659 3%

137 ->138 -0.33586 22%

137 ->139 0.59516 70%

The first three excited electronic states for the Py-Ph-BD1 system in dichloroethane at the emission geometry.

Excited State 1: Singlet-A 2.5985 eV 477.15 nm f=0.6594 <S**2>=0.000

136 ->138 -0.68399 94%

136 ->139 0.15854 5%

Excited State 2: Singlet-A 2.6157 eV 474.00 nm f=1.2232 <S**2>=0.000

133 ->138 -0.12782 3%

135 ->138 0.11793 3%

137 ->138 0.65473 85%

137 ->139 0.17329 6%

Excited State 3: Singlet-A 3.4919 eV 355.07 nm f=0.3610 <S**2>=0.000

133 ->138 0.14316 4%

135 ->138 -0.12928 3%

137 ->138 -0.11662 3%

137 ->139 0.66061 87%

The first three excited electronic states for the Py-Ph-BD2 system in DCE at the absorption geometry.

Excited State 1: Singlet-A 2.6363 eV 470.30 nm f=0.8191 <S**2>=0.000

153 ->154 0.70115 98%

Excited State 2: Singlet-A 3.6969 eV 335.37 nm f=0.7097 <S**2>=0.000

148 ->154 0.17392 6%

152 ->154 0.49119 48%

152 ->155 -0.45371 41%

Excited State 3: Singlet-A 3.7368 eV 331.79 nm f=0.1005 <S**2>=0.000

150 ->154 0.70035 98%

The first three excited electronic states for the Py-Ph-BD2 system in DCE at the emission geometry.

Excited State 1: Singlet-A 2.5078 eV 494.39 nm f=0.7070 <S**2>=0.000

152 ->154 -0.68215 93%

152 ->155 0.16424 5%

Excited State 2: Singlet-A 2.6246 eV 472.39 nm f=1.2551 <S**2>=0.000

148 ->154 -0.12441 3%

151 ->154 0.12367 3%

153 ->154 0.65482 86%

153 ->155 0.17232 6%

Excited State 3: Singlet-A 3.3660 eV 368.34 nm f=0.0508 <S**2>=0.000

150 ->154 0.68163 93%

150 ->155 -0.16490 5%

The first three excited electronic states for the Py-Ph-BD1 system in ACN at the absorption geometry.

Excited State 1: Singlet-A 2.6807 eV 462.51 nm f=0.8043 <S**2>=0.000

136 ->138 0.70151 98%

Excited State 2: Singlet-A 3.6576 eV 338.97 nm f=0.5302 <S**2>=0.000

133 ->138 0.19826 8%

137 ->138 0.54351 58%

137 ->139 0.38264 29%

Excited State 3: Singlet-A 3.7825 eV 327.78 nm f=0.6439 <S**2>=0.000

133 ->138 -0.13577 4%

137 ->138 -0.35250 25%

137 ->139 0.58447 68%

The first three excited electronic states for the Py-Ph-BD1 system in ACN at the emission geometry.

Excited State 1: Singlet-A 3.4993 eV 354.31 nm f=0.6132 <S**2>=0.000

133 ->138 0.22137 10%

135 ->138 0.10028 2%

136 ->138 0.59119 70%

136 ->139 0.28216 16%

Excited State 2: Singlet-A 2.5685 eV 482.70 nm f=0.7635 <S**2>=0.000

137 ->138 0.70014 98%

Excited State 3: Singlet-A 3.8209 eV 324.49 nm f=0.0324 <S**2>=0.000

134 ->138 0.65762 86%

136 ->139 0.20814 9%

The first three excited electronic states for the Py-Ph-BD2 system in ACN at the absorption geometry.

Excited State 1: Singlet-A 2.5993 eV 476.99 nm f=0.8561 <S**2>=0.000

153 ->154 0.70136 98%

Excited State 2: Singlet-A 3.6757 eV 337.30 nm f=0.7724 <S**2>=0.000

148 ->154 0.17032 6%

152 ->154 0.47971 46%

152 ->155 -0.46851 44%

Excited State 3: Singlet-A 3.7308 eV 332.32 nm f=0.0990 <S**2>=0.000

150 ->154 0.70092 98%

The first three excited electronic states for the Py-Ph-BD2 system in ACN at the emission geometry.

Excited State 1: Singlet-A 2.4756 eV 500.82 nm f=0.7455 <S**2>=0.000

152 ->154 -0.68230 92%

152 ->155 0.16385 5%

Excited State 2: Singlet-A 2.5763 eV 481.26 nm f=1.2952 <S**2>=0.000

148 ->154 -0.12295 3%

151 ->154 0.12436 3%

153 ->154 0.65437 85%

153 ->155 0.17423 6%

Excited State 3: Singlet-A 3.3560 eV 369.44 nm f=0.0529 <S**2>=0.000

150 ->154 0.68274 93%

150 ->155 -0.16230 5%

A CS state is also predicted by TD-DFT calculations as shown in Figure S20 using the G09 computational package. More precisely, optimization of the **Py-Ph-BD1** geometry results in a structure where the plane of the phenyl ring is nearly perpendicular to both chromophoric fragments i.e., the planes of pyrene and **BD1**. Using the M06-2X functional, and the 6-31G(d,p) basis set, we obtain two distinct absorption peaks in the range from 300 to 550 nm, which are in reasonable agreement with the experiment (Figure S20). The peak calculated in the area that corresponds to pyrene absorption has contributions from both pyrene to bodipy and pyrene to pyrene excitations (Figure S20 and S21-S23). This is also found after geometry optimization of the excited state S_2 at the emission geometry for both dyads calculated in both solutions. Thus, the theoretical results indicate similar contributions of the CS state in the S_2 states of the dyads.

It might be noted that in the area where pyrene absorbs, calculations on bodipy alone find the second and third excited states of bodipy, lying close in energy but with different orientation in their dipole transition moments. Therefore, the broad, higher energy and low-intensity band of bodipy can be assigned to absorption to these states.

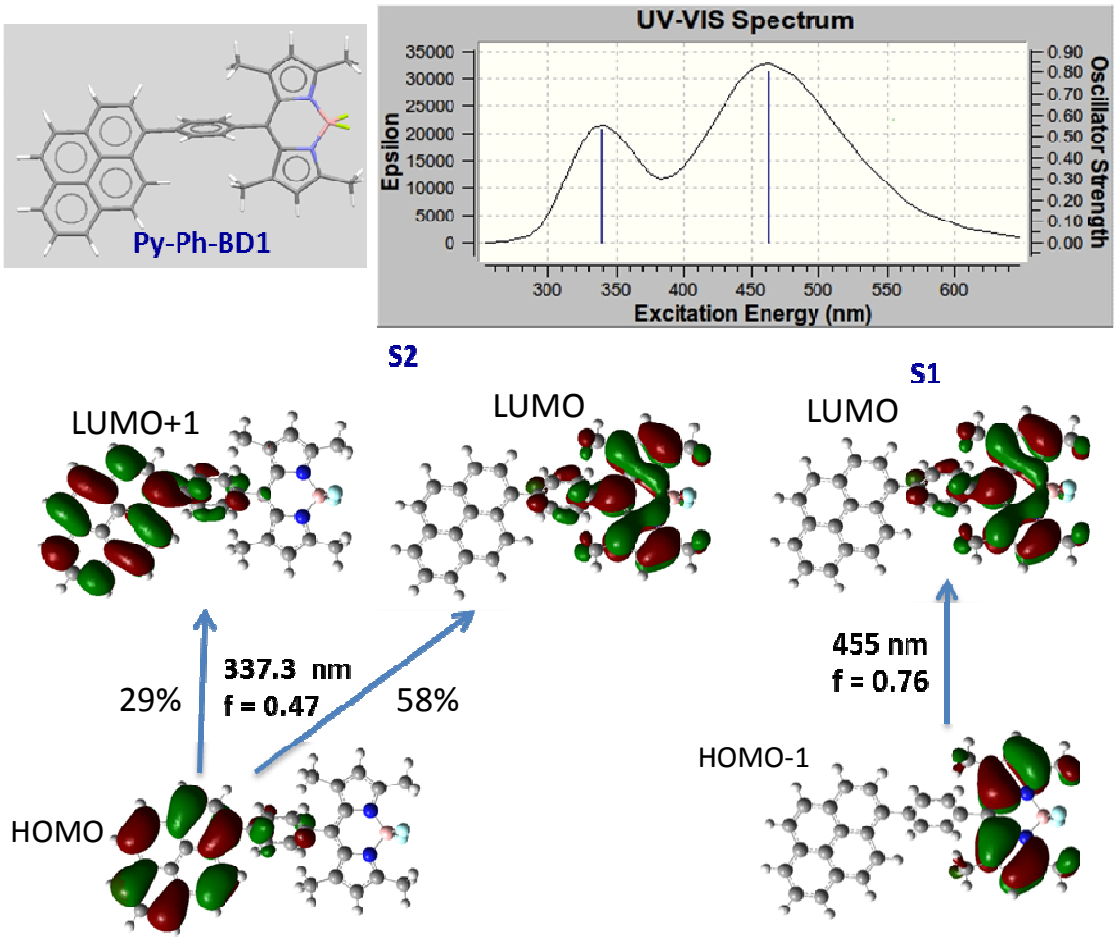

Figure S20. (Upper panel) Calculated absorption spectrum for the dyad **Py-Ph-BD1** in ACN. (Low panel) Analysis of dominant excitations in terms of the two highest occupied (HOMO, HOMO-1), and two lowest unoccupied (LUMO, LUMO+1) molecular orbitals (MOs).

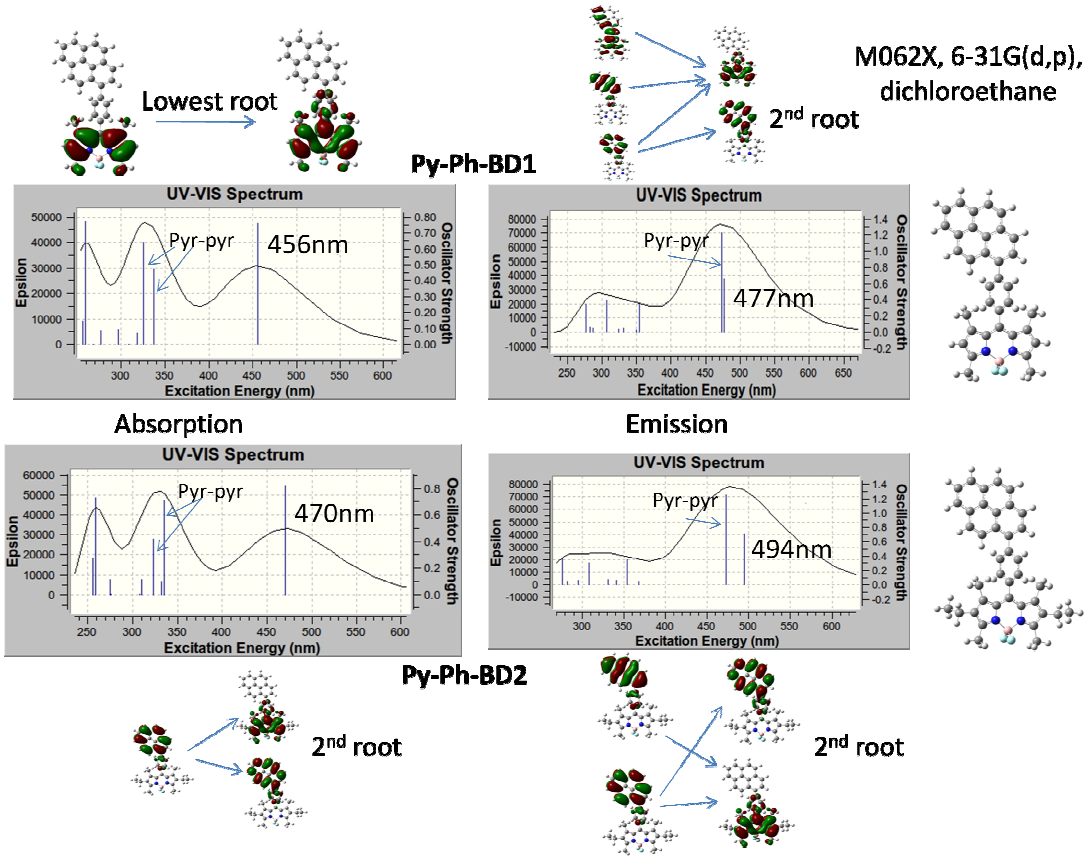

Figure S21. Absorption and emission spectra from TD-DFT calculations using the M062x functional and the 6-31G(d,p) basis set in DCE solution, searching for the first 10 roots for the **Py-Ph-BD1** and the **Py-Ph-BD2** systems.

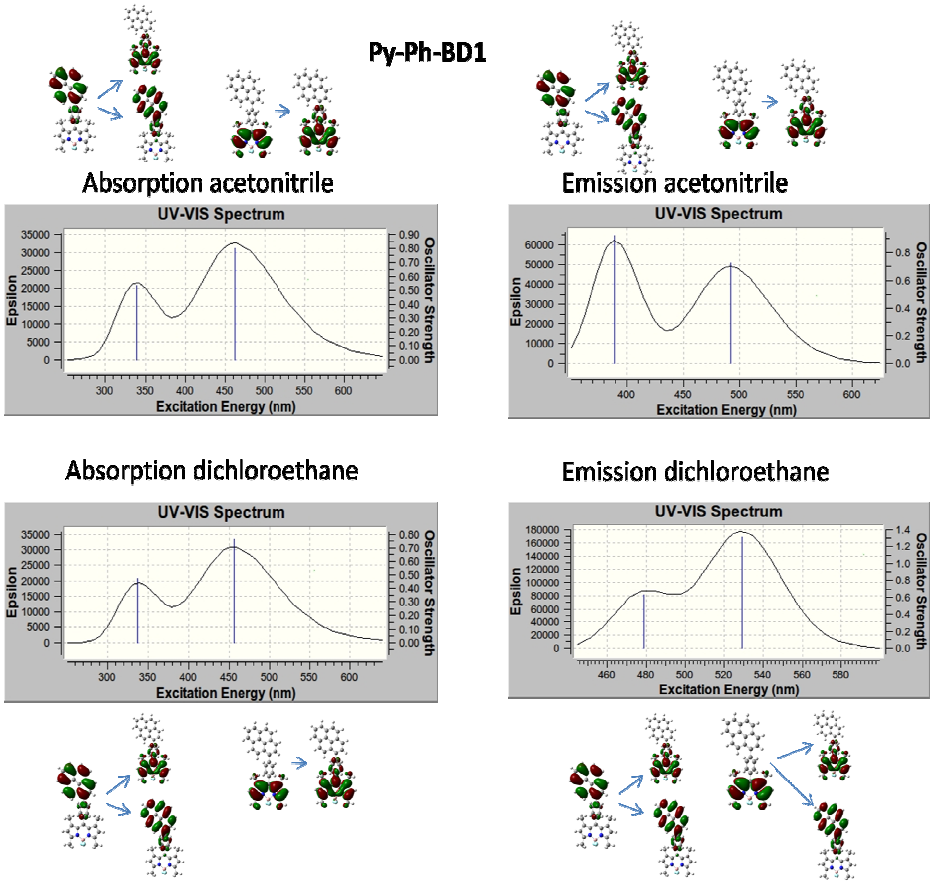

Figure S22. Absorption and emission spectra from TD-DFT calculations using the M062x functional and the 6-31G(d,p) basis set in DCE and ACN solutions, searching for the first 2 roots (for clarity) for the **Py-Ph-BD1** system.

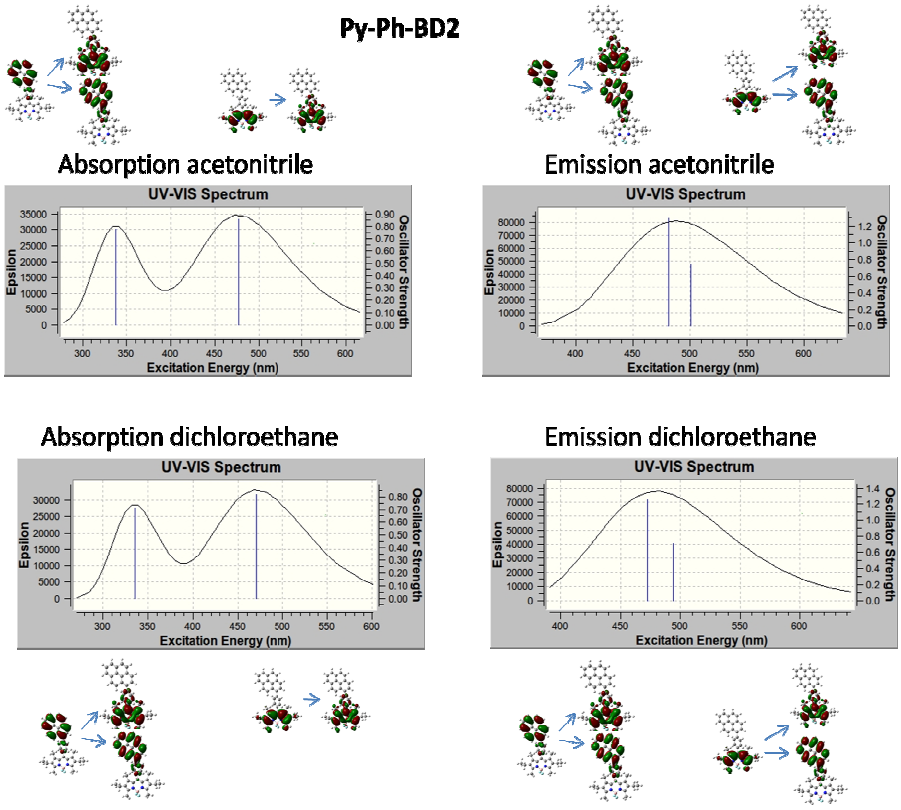

Figure S23. Absorption and emission spectra from TD-DFT calculations using the M062x functional and the 6-31G(d,p) basis set in DCE and ACN solutions, searching for the first 2 roots (for clarity) for the **Py-Ph-BD2** system.

References.

S1. M. Beinhoff, W. Weigel, M. Jurczok, W. Rettig, C. Modrakowski, I. Brüdgam, H. Hartl, A. D. Schlüter, *Eur. J. Org. Chem.,* 2001, **66**, 3819-3829.

S2. M. Shah, K. Thangaraj, M. L. Soong, L. T. Wolford, J. H. Boye, I. R. Politzer, T. G. Pavlopoulos, *Heteroatom Chem., 1990*, ***1***, 389-399.

S3. Y. Gabe, Y. Urano, K. Kikuchi, H. Kojima and T. Nagano, *J. Am. Chem. Soc.,* 2004, **126**, 3357-3367.

S4. T. N. Singh-Rachford, A. Haefele, R. Ziessel and F. N. Castellano, *J. Am. Chem. Soc.,* 2008, **130**, 16164-16165.

S5. T. Pullerits, S. Hess, J. L. Herek and V. Sundström, *J. Phys. Chem. B*, 1997, **101**, 10560-10567.

S6. Molecular Fluorescence: Principles and Applications. Bernard Valeur 2001 Wiley-VCH Verlag GmbH.

S7. R. G. Alden, E. Johnson, V. Nagarajan, W. W. Parson, C. J. Law and R. G. Cogdell, *J. Phys. Chem. B*, 1997, **101**, 4667-4680.

S8. A. Weller, Z. *Phys.-Chem. Materialforcsh.*, 1982, **133**, 93.

S9. Y Gabe, Y. Urano, K. Kikuchi, H. Kojima and T. Nagano, *J. Am. Chem. Soc.*, 2004, **126**, 3357-3367.